

ARMY RESEARCH LABORATORY



Molecular Dynamics Investigation of the Desensitization of Detonable Material

by Betsy M. Rice, William Mattson,
and Samuel F. Trevino

ARL-TR-1744

August 1998

19980923 033

Approved for public release; distribution is unlimited.

DTIC QUALITY INSPECTED 1

The findings in this report are not to be construed as an official Department of the Army position unless so designated by other authorized documents.

Citation of manufacturer's or trade names does not constitute an official endorsement or approval of the use thereof.

Destroy this report when it is no longer needed. Do not return it to the originator.

Army Research Laboratory

Aberdeen Proving Ground, MD 21005-5066

ARL-TR-1744

August 1998

Molecular Dynamics Investigation of the Desensitization of Detonable Material

Betsy M. Rice, William Mattson, Samuel F. Trevino
Weapons and Materials Research Directorate, ARL

Abstract

A molecular dynamics investigation of the effects of a diluent on the detonation of a model crystalline explosive is presented. The diluent, a heavy material that cannot exothermally react with any species of the system, is inserted into the crystalline explosive in two ways. The first series of simulations investigates the attenuation of the energy of a detonation wave in a pure explosive after it encounters a small layer of crystalline diluent that has been inserted into the lattice of the pure explosive. After the shock wave has traversed the diluent layer, it reenters pure explosive. Unsupported detonation is not reestablished unless the energy of the detonation wave exceeds a threshold value. The second series of simulations investigates detonation of solid solutions of different concentrations of explosive and diluent. For both types of simulations, the key to reestablishing or reaching unsupported detonation is the attainment of a critical number density behind the shock front. Once this critical density is reached, the explosive molecules transition to an atomic phase. This is the first step in the reaction mechanism that leads to the heat release that sustains the detonation. The reactive fragments formed from the atomization of the heteronuclear reactants subsequently combine with new partners, with homonuclear product formation exothermally favored.

Table of Contents

	<u>Page</u>
List of Figures	v
1. Introduction	1
2. Model	3
3. Details of the Calculations	4
3.1 Slab Experiments	7
3.2 Solid Solution	8
4. Results	9
4.1 Slab Simulations	9
4.2 Solid-Solution Simulations	14
5. Conclusions	15
6. References	17
Distribution List	19
Report Documentation Page	27

INTENTIONALLY LEFT BLANK.

List of Figures

<u>Figure</u>	<u>Page</u>
1. Representations of Lattice Models Used in the Simulations: (a) Pure Explosive or Solid Solution and (b) Pure Explosive With Layer of Diluent Molecules Inserted Into the Crystal Lattice	5
2. Schematics of the Models Used in the Molecular Dynamics Simulations of Explosive/Diluent Crystals	6
3. Position of the Shock Front as a Function of Time for Explosives With Layers of Diluent That Have Widths of (a) 69 Å, (b) 87 Å, (c) 95 Å, (d) 104 Å, and (e) 138 Å	10
4. Atomic Number Density as a Function of Position Along the x Direction of the Model at (a) 8.5 ps, (b) 9.0 ps, (c) 12.0 ps, and (d) 14.5 ps	12
5. Atomic Number Density as a Function of Position Along the x Direction of the Model at (a) 8.5 ps, (b) 9.0 ps, (c) 12.0 ps, and (d) 14.5 ps	13

INTENTIONALLY LEFT BLANK.

1. Introduction

The process known as detonation has received considerable attention for its unique chemistry and physics and its military and industrial applications. Many explosives are well characterized at the macroscale and are adequately described at this level by hydrodynamic theories [1, 2]. However, atomic-level details of detonation are not completely resolved, resulting in a gap in information that could otherwise be exploited in designing energetic materials with controlled detonation characteristics. This information includes features of the mechanisms of the chemical reactions and energy transfer that drive the detonation wave and conditions that affect these mechanisms. Much has been written concerning the first step in reactions of an explosive to produce a detonation wave [3, 4]. Traditional views of the first step have assumed rupture of the weakest bond of the energetic molecule by thermal activation and/or mechanical stripping of fragments. Subsequently, the reactive species combine chemically and release energy to sustain the detonation. More recently, metallization has been invoked as a possible rate-controlling mechanism in the initial step [5]. Experimental data that could identify these various mechanisms are not available due to the small time and spatial scales over which detonation occurs. Typical detonation waves propagate through condensed media at speeds ranging from 1 to 10 km/s (1–10 nm/ps) and are currently outside the scope of experimental probe. Measurement is further complicated by the extreme energy and pressure release. The experimental community has made extensive progress toward measurement of detonation at subnanoscale regimes [4], but the necessary scale has yet to be reached.

Information at the microscale is readily obtained from molecular simulation. Through it, the viewer observes and measures the dynamic events associated with detonation at the appropriate time and spatial scales. The motion of and force experienced by each particle in such a simulation can be monitored over time, allowing the investigator to witness reaction mechanisms. Several molecular dynamics studies of shock-induced reaction waves in energetic molecular crystals show that detonation can be simulated using the method of molecular dynamics [6–25]. The main limitation of such studies to date, however, is the highly idealized representation of the energetic molecular system. Many common explosives are large, polyatomic, organic molecules; and the

reactions leading to detonation are thought to consist of several steps leading to the heat release that sustains the reaction wave. Most systems used in molecular simulations are simple di- and triatomic molecular crystals, and the heat-release reaction usually involves no more than two steps [6–25]. Despite these limitations, the simulations using such models have been extremely successful in reproducing characteristics of a detonation. In particular, the models of explosives developed by White and co-workers represent the chemistry thought to occur in detonation, and explicitly include many-body effects [17, 18]. These models, which use a modified Tersoff [26, 27] form to describe the inter- and intramolecular interactions, have been successfully used to simulate chemically sustained reaction waves in crystals [16–18, 20–25]. Such successes can be augmented by using information gained from simulations to design an energetic material with specific performance properties. The present study explores this possibility, using results from previous molecular dynamics investigations of detonation [20, 21]. It was found that the first step in the reaction sequence leading to detonation is the compression of the energetic solid to a critical density [20]. The simulations show that detonation will result if the critical density of the energetic material is reached. A reasonable inference would be that the energetic material can be tailored such that this critical density will not be reached, except under specific and controlled conditions. Tailoring toward desensitization could occur through the addition of inert dopants or defects, which would influence the degree of compression of the explosive due to shock wave passage. The work reported here explores this hypothesis.

We present results from molecular dynamics simulations that investigate the effect on detonation of an explosive by the addition of an inert, heavy diluent. This diluent is inserted into the explosive crystal in either a layered fashion (slab simulations) or as part of a solid solution (solid-solution simulations). The “slab” simulations investigate the conditions necessary for a slab of inert material inserted into the lattice to quench a detonation wave propagating through a pure explosive. The solid-solution simulations investigate the behavior of mixtures of explosive and diluent after shock initiation. Finally, the dependence of detonation on the degree of compression of the material is determined.

2. Model

The models in this study are all two-dimensional (2-D), and consist of diatomic molecules arranged in herringbone lattices. The explosive molecules are denoted hereafter as "A-B" and the diluent molecules will be denoted as "C₂". All particles in the system interact through the following interaction potential, a modified form of that developed in Brenner et al. [17, 18]:

$$V = \sum_i^N \sum_{j>i}^N \left\{ f_c(r_{ij}) \left[(2 - \overline{B}_{ij}) V_R(r_{ij}) - \overline{B}_{ij} V_A(r_{ij}) \right] + V_{vdw} \right\}. \quad (1)$$

Parameters for the function and a description of the properties of this interaction potential are given in Rice et al. [20, 21]. The V_R and V_A terms are functions that describe intramolecular repulsions and attractions, respectively. The V_{vdw} term describes nonbonding interactions. A many-body term, denoted as \overline{B}_{ij} , modifies the intramolecular interactions of a pair of atoms, i and j , according to the distribution of atoms surrounding the i - j pair. The value of \overline{B}_{ij} ranges from 0 to 1 and depends only on the arrangement of atoms surrounding each atom pair. The value of \overline{B}_{ij} does not depend on the atom type. The form of this potential attenuates the attractive intramolecular interaction and increases the repulsive interaction as an atom pair experiences an increasingly dense local environment, such as that occurring through shock wave passage. The previous study [21] showed that, in the reaction zone (the region behind the shock front in which the A-B molecules had not yet reacted), the density was such that the atom pairs within each A-B molecule were experiencing no attractions. Thus, the molecules became "unbound" due to the compression of the material by passage of the pressure wave. Once the shock wave passed and density of the region decreased, the attenuation of intramolecular attractions subsided and the nascent atoms were free to combine with new partners. For this system, homonuclear product formation is energetically favored, and formation of such provides the energy needed to sustain the detonation wave.

In the low-temperature, low-pressure, crystal structure, bond strengths of the A-B, A₂, and B₂ molecules are 1, 5, and 2 eV, respectively. The C atom has the same interaction potential with all other species in the system as the A atom. The only difference between the C and A atoms is the

mass. The mass of the C atom (150 amu) is 10 times that of the A atom (15 amu). The bond strength of an isolated C₂ molecule is 5 eV, making it more stable than reactants by 4 eV. Also, the C₂ molecule has the same internuclear bond distance as the A₂ molecule (1.2 Å). The C₂ molecule can be dissociated with sufficient energy. However, there is no net energy change upon formation of C-A or recombination to form C₂. Also, formation of C-B is endothermic. Thus, C₂ is appropriate as an “inert” diluent for desensitization of the model A-B explosive. The exothermic reactions for this system are:



and



Due to the form of the interaction potential in equation (1), the C atom can influence the intramolecular interactions experienced by atom pairs in this system. Thus, atom pairs within a mixture of diluent and explosive described by this form of potential energy function will experience similar modifications of intramolecular forces upon compression, as seen in the pure explosive.

3. Details of the Calculations

Details of the molecular dynamics simulations of the tailored explosives are the same as those described in Rice et al. [section III.D., 20]. The most significant difference in the simulations is that the models do not consist of pure explosive but include the diluent C₂ molecules. Figure 1 represents the lattice models used in this study. For all simulations, all atoms in the simulation box are arranged in the local equilibrium position associated with the herringbone lattice. Atoms in the equilibrium herringbone arrangement are illustrated in Figure 2. The upper frame of Figure 2 shows the equilibrium herringbone lattice for a solid solution of A-B explosive mixed with diluent C₂ molecules; the pure explosive crystal has the same atomic arrangement and differs only in the chemical composition (see Figure 1 of Rice et al. [20]). Each atom is given kinetic energy (KE) totaling 20 K partitioned equally between the x- and y-momentum components. The equations of

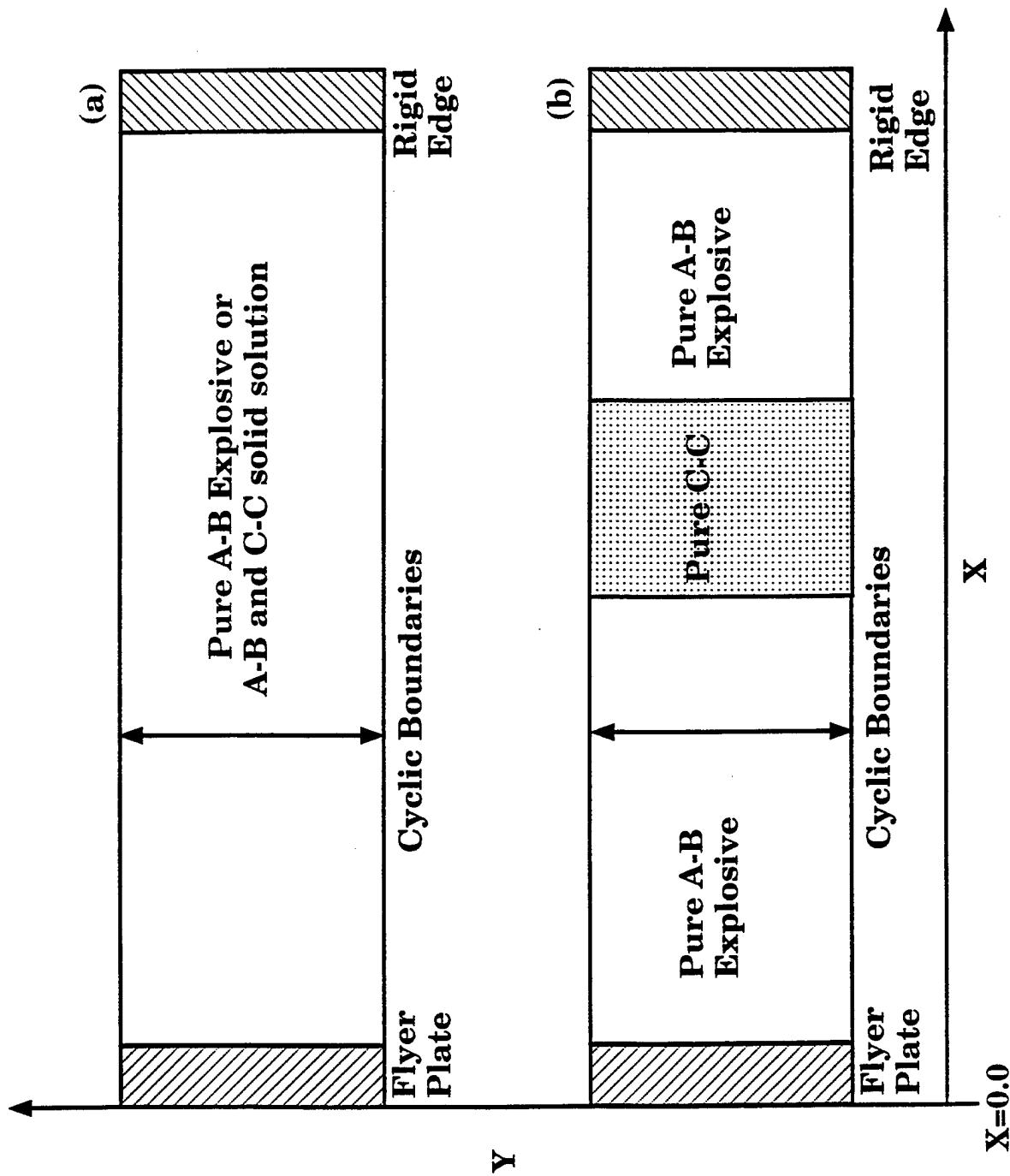


Figure 1. Representations of Lattice Models Used in the Simulations: (a) Pure Explosive or Solid Solution and (b) Pure Explosive With Layer of Diluent Molecules Inserted Into the Crystal Lattice.

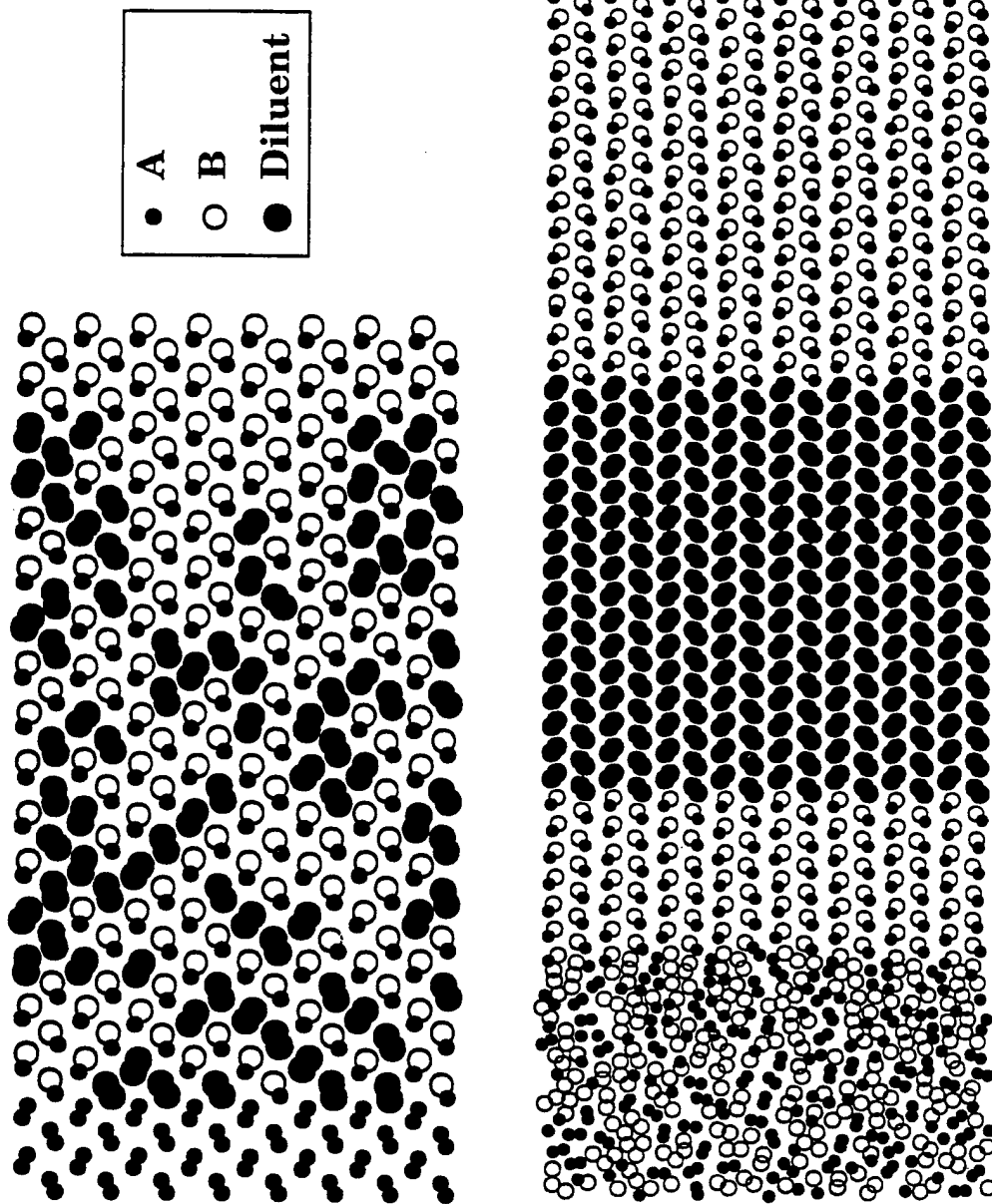


Figure 2. Schematics of the Models Used in the Molecular Dynamics Simulations of Explosive/Diluent Crystals. Atom Type A (Mass = 15 amu) Is Denoted by Small Filled Circles, Atom Type B (Mass = 46 amu) Is Denoted by Open Circles, and Atom Type C (Mass = 150 amu) Is Denoted by Large, Filled Circles. The Upper Frame Shows Solid Solution of the Initial Positions of Explosive and Diluent. The Concentration of Diluent Is 37.5%. The Lower Frame Shows a Snapshot of the Layered Explosive/Diluent at 5.6 ps, Immediately Before the Detonation Wave Reaches the Left Edge of the Diluent Region. The Width of the Diluent Slab is 69 Å.

motion for the atoms in the simulation box are integrated for 0.05 ps to allow for randomization of the energy in the crystal. A shock wave is then initiated by the impact of a thin flyer plate consisting of 64 A_2 molecules moving at a velocity of 12 km/s. The earlier work [20] showed that a flyer plate of this size, chemical composition, and velocity is sufficient to achieve steady detonation of the pure explosive. The shock wave initiates at the far left edge of the simulation cell and propagates to the right. The model has cyclic boundary conditions in the y direction but is terminated by a slab of rigid A-B molecules at the far right edge of the material. The model is not bound at the left edge but can expand in the negative-x direction as the flyer plate rebounds and the rarefaction occurs. The temperature of the crystal through which the shock wave will propagate is 20 K.

As in the previous study [20], the simulations here use the expanding computational window technique first developed by Tsai and Trevino [6, 7]. The temperature within an $8.68\text{-}\text{\AA} \times 50.16\text{-}\text{\AA}$ section of the crystal located $60.76\text{ }\text{\AA}$ from the far-right edge of the terminating cell is monitored at each integration step. When the temperature within this “test” region exceeds that of the undisturbed crystal by 50%, it is assumed that the shock wave has propagated into this region. At that point, an $8.68\text{-}\text{\AA} \times 50.16\text{-}\text{\AA}$ section of crystal is inserted immediately before the rigid, terminating cell. The atoms in the new segment are arranged in the equilibrium herringbone lattice position, and energy totaling 20 K is partitioned into the x- and y-momentum components of each atom. The trajectory integration continues, with crystal added as needed to study wave propagation.

In the previous work [20], the shock front corresponded to the right-most point along the x axis in which the mass density was greater than that of undisturbed A-B crystal. This definition of shock front position is inadequate for this study, since the mass density of the slab at the low pressure equilibrium ($22.1\text{ amu}/\text{\AA}^2$) greatly exceeds that of shocked A-B explosive ($<10\text{ amu}/\text{\AA}^2$). For this study, the shock front is the rightmost $2.17\text{ }\text{\AA} \times 50.16\text{ }\text{\AA}$ section along the x axis of the model in which the average KE of the atoms exceeds 50 K. This prescription proved to be both more sensitive and stable than, say, using number density.

3.1 Slab Experiments. The first series of simulations exploits ideas used in measurements of explosive sensitivity known as “gap tests” [28]. These tests involve initiating a charge separated

from the explosive being tested by an attenuating material. The shock wave produced from the initiating charge passes through the attenuating material before entering the sample explosive. The sensitivity of the explosive is defined in terms of the width of the attenuating material required for a 50% probability of initiation. Obviously, a slab of infinite width would completely attenuate the energy of the shock wave and the sample explosive would never detonate. The simulations reported in this work investigate the quenching of a detonation using such an attenuating material as a function of width.

The models consist of pure A-B crystal except for a slab of material composed of C_2 molecules inserted into the explosive crystal. Pure explosive (with no defects) is on either side of the slab of C_2 molecular crystal (Figure 2). After flyer-plate initiation, detonation of the pure explosive is allowed to reach steady state before the front reaches the slab of C_2 molecules. For each simulation, the shock front will reach the slab region at 6.0 ps after shock initiation. The propagating detonation wave traverses the C_2 slab and then enters another region of pure explosive. The reactions behind the shock wave after traversing the diluent region are monitored to decide if detonation is reestablished. Five simulations that vary in the width of the slab of C_2 molecules are performed. All of the slabs run the length of the simulation cell in the y direction (50.16 Å) and have periodic boundary conditions in that dimension. The differences in the sizes of the slabs are due to the width in the x direction. The widths of the slabs are 69.4, 86.8, 95.5, 104.2, and 138.9 Å. These simulations are denoted hereafter by the width of the slabs (i.e., 69, 87, 95, 104, and 139 Å).

3.2 Solid Solution. The second set of computer simulations explores the response of explosive/diluent solutions upon flyer-plate impact. The A-B explosive is mixed with the previously described C_2 molecules to form solid solutions. Three solutions are chosen, with 31.25%, 34.375%, and 37.5% concentration of C_2 molecules. The simulations are denoted from now on by concentration of C_2 . The model of the solid solution is prepared as follows: the simulation cell at the beginning of the trajectory has dimensions of $69.44 \text{ Å} \times 50.16 \text{ Å}$, and the cell is partitioned into rectangular sections with dimensions of $8.68 \text{ Å} \times 50.16 \text{ Å}$. A section of crystal with these dimensions can hold exactly 32 diatomic molecules in the low-pressure, equilibrium, herringbone, lattice arrangement. The chemical composition of the 32 diatomic molecules (i.e., A-B or C_2) is

assigned randomly according to the desired percent concentration of diluent molecules. Before the flyer plate is allowed to strike the edge of the simulation box of explosive/diluent mixture, the system is allowed to relax through a 0.05-ps warmup, molecular dynamics simulation. Energy redistribution and equipartitioning between the potential and kinetic energies are ensured by monitoring these during the warmup trajectory. After the warmup trajectory, the thin flyer plate of A_2 molecules moving with a velocity of 12 km/s strikes one edge of the solid solution. As the shock wave propagates into undisturbed crystal, the simulation cell expands by the addition of a rectangular section of the solid solution, whose chemical composition has a fixed concentration of C_2 molecules arranged randomly, as described previously.

4. Results

4.1 Slab Simulations. The velocity of the shock wave of an unsupported detonation is a property of the explosive [1, 2]. For pure A-B explosive, the velocity of the detonation wave once steady state has been reached is 6.6 km/s [20]. Thus, the velocity of the shock wave through the explosive after traversing the slab of diluent is an indicator of whether detonation is reestablished. Figure 3 shows the positions of the shock fronts as functions of time for the simulations. The slopes of these curves correspond to the velocities of the propagating waves. The slope of each curve from 0.5 to 6 ps is 6.6 km/s. At 6 ps, the shock front enters the slab of C_2 molecules. The horizontal arrow in each frame of Figure 3 shows the interval over which the shock front is in the slab of diluent molecules. The slope of each curve during this interval is less than that at the earlier interval of 0.5–6 ps, showing that the shock wave is propagating more slowly. The times in the trajectories at which the fronts reenter explosive are 7.8, 8.2, 8.4, 8.7, and 9.7 ps for the 69-, 87-, 95-, 104-, and 138-Å slab simulations, respectively. Linear, least-squares fits of the curves from 12 to 15 ps give shock wave velocities of 6.8, 6.6, 6.7, 4.4, and 4.3 km/s for the 69-, 87-, 95-, 104-, and 138-Å simulations, respectively. The three simulations in which the shock velocities reach 6.6 km/s in the pure A-B explosive after traversing the diluent slab show that detonation is reestablished. Detonation of the A-B explosive did not resume after the shock wave traversed the slabs of C_2 molecules with widths of 104 and 138 Å.

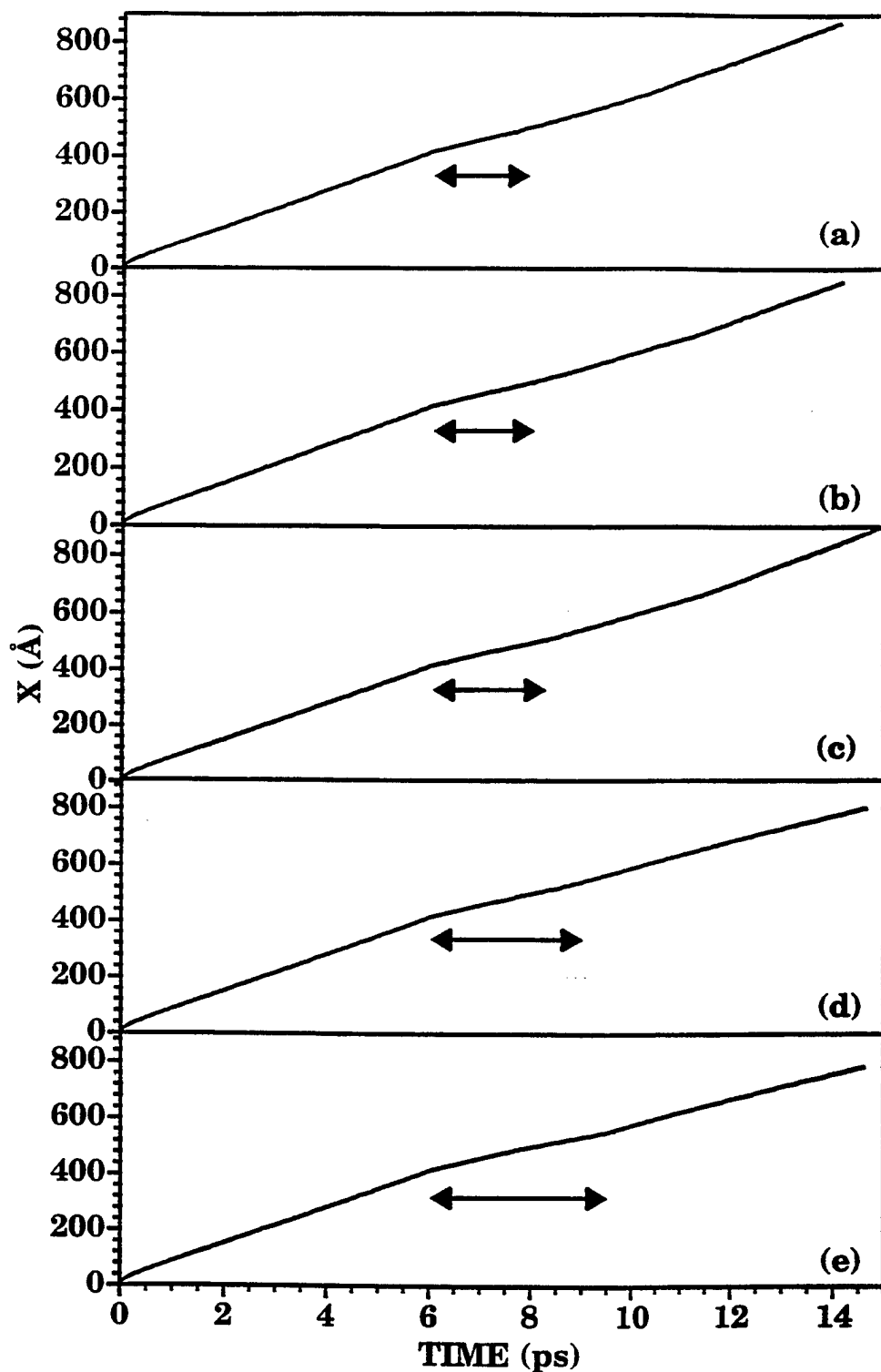


Figure 3. Position of the Shock Front as a Function of Time for Explosives With Layers of Diluent That Have Widths of (a) 69 Å, (b) 87 Å, (c) 95 Å, (d) 104 Å, and (e) 138 Å. The Horizontal Line in Each Frame Illustrates the Time Interval of the Trajectory Over Which the Shock Front Is in the Layer of Diluent Molecules.

Figures 4 and 5 show atomic number densities along the x axis at different times in the 104- and 95-Å simulations, respectively. As described in Rice et al. [20], a reactant A-B molecule is considered reacted if its internuclear distance exceeds 3.0 Å, the range of the intramolecular interaction potential. The designation of products in the figures merely means that the original A-B partners are no longer within the range of intramolecular interaction as defined by the function in equation (1). However, this test does not identify the products (homonuclear or heteronuclear diatomics or free atoms). Figure 4a shows atomic species profiles at 8.5 ps, soon after the time the shock front is reentering pure explosive after traversing the C₂ slab. In Figure 4b (0.5 ps later), no products have formed in the region beyond the diluent slab. In both Figures 4a and b, the diluent slab is compressed to ~75% of its low-pressure, equilibrium width. The species profiles at 12 ps (Figure 4c) show that the diluent slab has expanded to approximately its original width (104 Å) and a few products have formed in the region immediately to its right. However, the shock discontinuity is over 100 Å ahead of the location of the products and is followed by unreacted A-B molecules. The species profiles in Figure 4d show that the distance between the positions of the shock discontinuity and the products along the x direction has increased over a 2.5-ps interval. Also, additional product has formed, and the diluent slab has undergone further expansion. Product formation immediately ahead of the diluent slab is most likely due to the compression of explosive on both sides. Compression from the left is due to expansion of the diluent slab after shock wave passage. Compression from the right is due to disturbed A-B explosive, whose rarefaction is blocked by the heavy slab of diluent molecules. The compression of explosive results in the initiating step of reaction for this system (i.e., atomization due to high density) followed by association to form exothermally favored, homonuclear products. However, the heat release from product formation is apparently far enough behind the shock front that it does not contribute to continued propagation of the shock wave.

A similar series of species profiles for the trajectory in which the width of the slab of C₂ molecules is 95 Å is shown in Figure 5. Figure 5a shows the profiles at 8.5 ps, near the point at which the shock wave is exiting the slab of C₂ molecules. The slab of diluent is compressed to ~80% of its low-temperature, low-pressure, equilibrium width. Figure 5b shows the species profile 0.5 ps later. Unlike the 104-Å trajectory at this point in the simulation, the diluent slab has expanded and

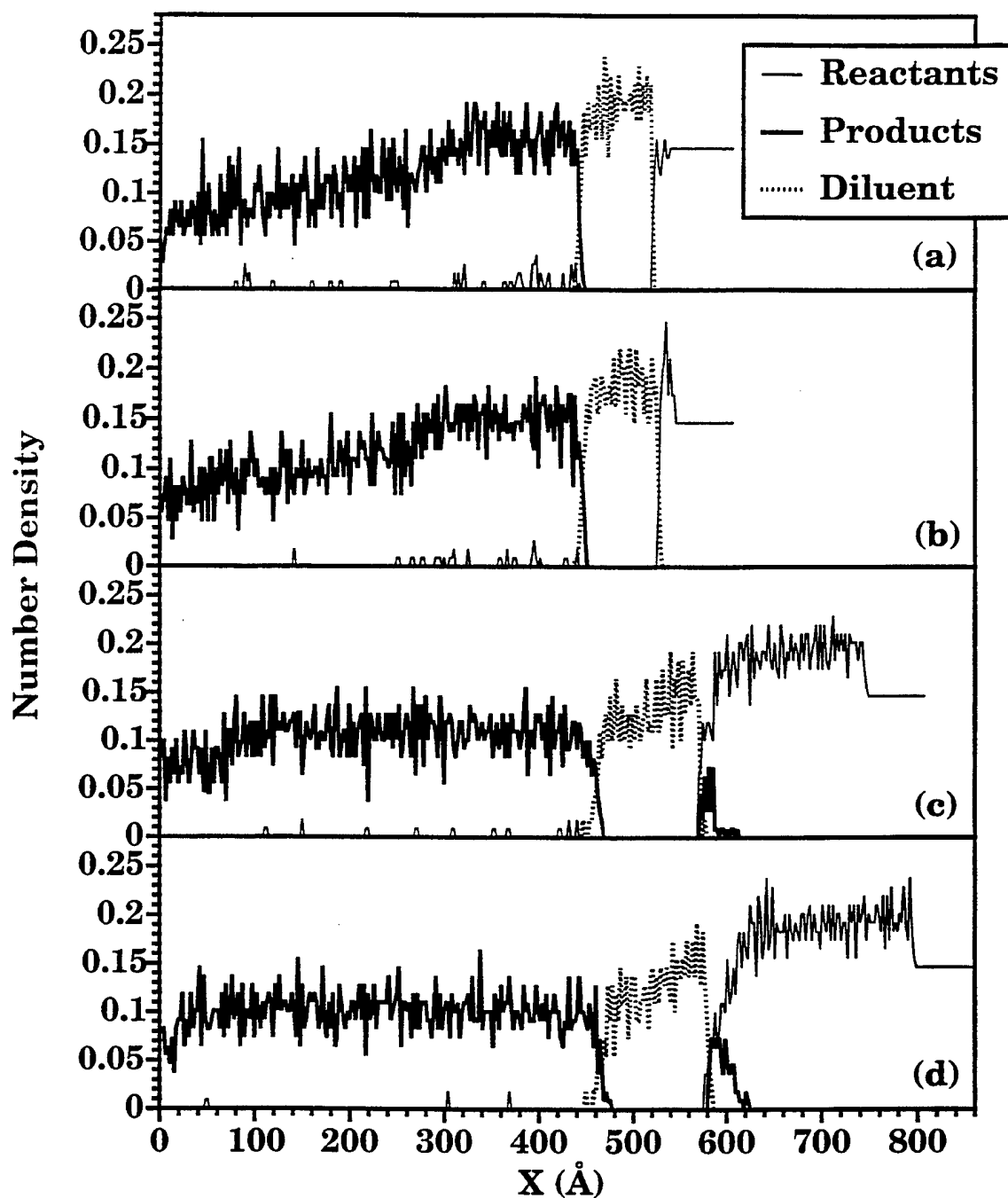


Figure 4. Atomic Number Density as a Function of Position Along the x Direction of the Model at (a) 8.5 ps, (b) 9.0 ps, (c) 12.0 ps, and (d) 14.5 ps. The Low-Pressure, Equilibrium Width of the Diluent Slab in This Simulation Is 104 Å. Units Are in Å⁻².

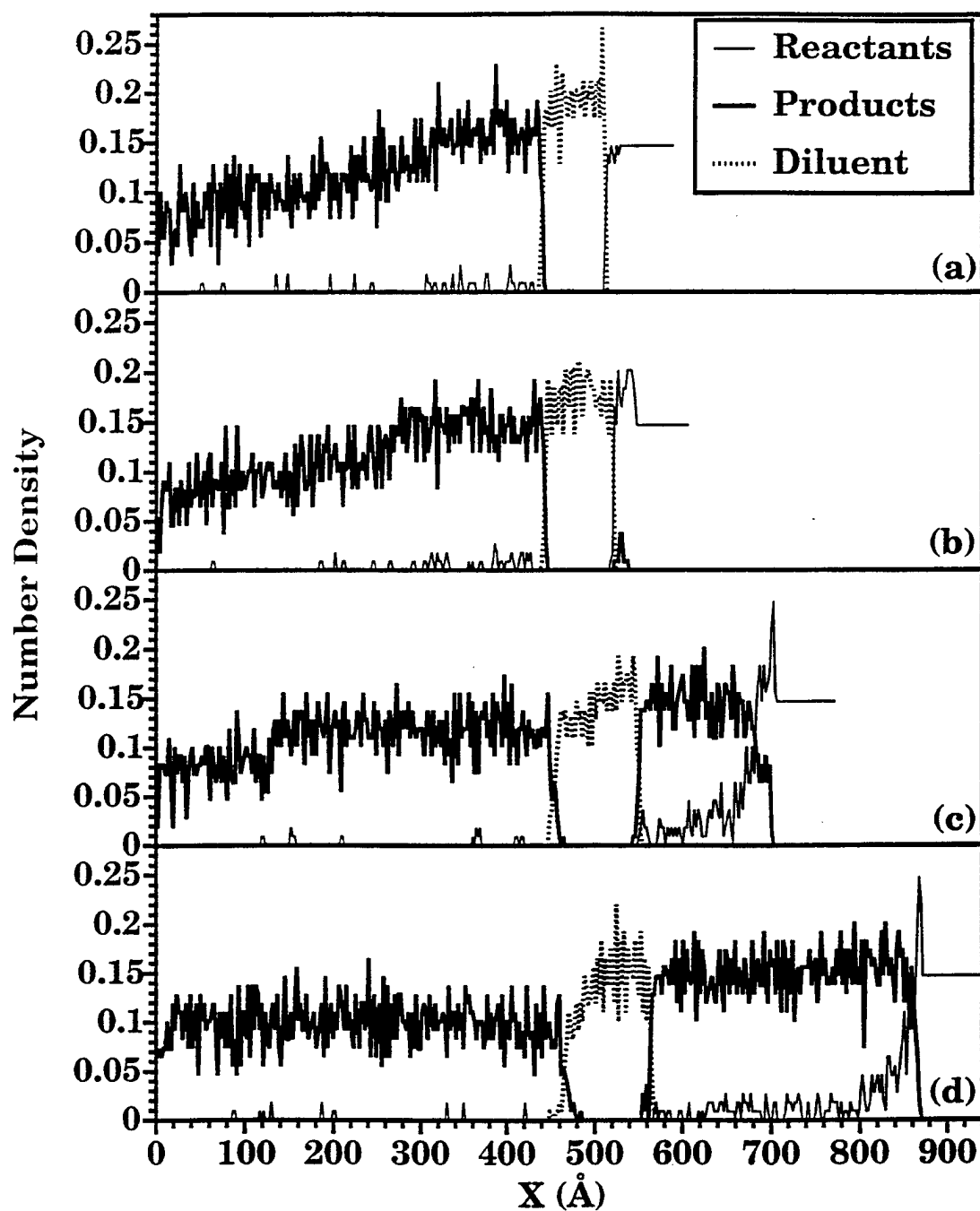


Figure 5. Atomic Number Density as a Function of Position Along the x Direction of the Model at (a) 8.5 ps, (b) 9.0 ps, (c) 12.0 ps, and (d) 14.5 ps. The Low-Pressure, Equilibrium Width of the Diluent Slab in This Simulation Is 95 Å. Units Are in Å⁻².

a few products have formed immediately behind the shock front. Substantial product formation almost directly behind the shock discontinuity is evident at the later times (Figures 5c and d), and the species profiles look similar to those corresponding to unsupported detonation in Rice et al. [20].

For those trajectories that reestablish detonation, the density behind the shock front reaches the Chapman-Jouguet value of the model explosive, which was shown in the previous work [20] to be the key to achieving sustained detonation. Examination of the results reveals that the critical density is not reached in the 104- and 138-Å simulations. For those cases, there is insufficient energy in the reentering shock wave to compress the explosive such that atomization and subsequent exothermic product formation will result. The energy of the detonation wave is attenuated as it traverses the heavy, diluent region, transferring energy into the stationary, heavy C_2 molecules. Since there is no possibility of exothermic reaction within the diluent, there is no additional chemical energy released to drive the propagating wave in this region. By the time the shock wave reaches the far-right edge of the diluent region, it is moving with a slower velocity (therefore, a smaller KE) than it had when it first entered that region. As shown in the flyer-plate simulations of pure explosive [20], there is a threshold energy needed to compress the pure explosive to the critical density. Apparently, a slab of diluent that is at least 104 Å wide is sufficient to dissipate the energy of the shock wave below the threshold value.

4.2 Solid-Solution Simulations. Two of the three solid solutions (those with concentrations of 31.25 and 34.375% C_2 molecules) result in an unsupported detonation. In the previous work [20], detonation is sustained if the number density of the material behind the shock front in the pure explosive reaches $0.22 \text{ atom}/\text{\AA}^2$.^{*} In the present study, solid solutions that attain this number density sustain detonation; the solid solution that did not achieve this value did not sustain detonation. Also, the reaction zones[†] for the two simulations that showed sustained detonation are 22–25 Å in width, ~10 Å wider than that of the pure explosive [20]. A possible explanation for the increased, reaction

^{*} In Rice et. al [20], the analysis was performed in terms of mass density. In the present study, analysis in terms of number density is more appropriate.

[†] In this work and in Rice et. al [20], the reaction zone is defined to be the region between the shock discontinuity and the point at which the number of products exceeds that of reactants.

zone width is that product formation is sterically hindered by the presence of the diluent. In the shock compressed material, the C_2 molecules participate in atomization of the A-B molecules to form the reactive fragments (according to equation [1]). However, exothermal association of the fragments of the reactant A-B molecules could be obstructed by C_2 molecules.

5. Conclusions

We have shown, using the method of molecular dynamics, simple ways in which a model explosive can be tailored with a diluent to desensitize the material. The material was designed to exploit the reaction mechanism of the model, which is atomization of the explosive due to high compression, followed by the exothermal association of the fragments. Since the first step of the reaction involves high compression of the explosive, ways to attenuate the compression wave were introduced into the system. The first series of simulations investigated inserting slabs of inert heavy molecules into the explosive to absorb energy of the detonation wave. The attenuated shock wave, upon reentering explosive, has insufficient energy to achieve the critical compression necessary to atomize the reactant molecules.

The second series of simulations investigated the effect on detonation due to the mixture of a diluent with the explosive. The results showed that the diluent absorbs energy of the shock wave needed to compress the material to a critical density. The results also suggested that the diluent sterically hinders the reactive fragments from exothermic product formation. These two effects resulted in quenching the reactions that sustain the detonation.

This study shows that results obtained from molecular dynamics can be used in design of materials with specific performance objectives. The previously reported molecular dynamics simulations of the pure explosive established the reaction mechanisms of the models [20, 21] and the study reported here explore manipulations of the material to affect those reaction mechanisms. Clearly, microscale information obtained from this kind of modeling will become a useful and integral tool in the design and formulation of explosives with desired detonation characteristics.

INTENTIONALLY LEFT BLANK.

6. References

1. Fickett, W., and W. C. Davis. *Detonation*. University of California Press, Berkeley, CA, 1979.
2. Fickett, W. *Introduction to Detonation Theory*. University of California Press, Berkeley, CA, 1985.
3. Liebenberg, D. H., R. W. Armstrong, and J. J. Gilman. "Structure and Properties of Energetic Materials." *Materials Research Society Symposium Proceedings*, vol. 296, Materials Research Society, Pittsburgh, PA, 1993.
4. Brill, T. B., T. P. Russell, W. C. Tao, and R. B. Wardle. "Decomposition, Combustion and Detonation Chemistry of Energetic Materials." *Materials Research Society Symposium Proceedings*, vol. 418, Materials Research Society, Pittsburgh, PA, 1995.
5. Gilman, J. J. *Phil. Mag. B*. Vol. 67, p. 207, 1993.
6. Tsai, D. H., and S. F. Trevino. *Journal of Chemical Physics*. Vol. 81, p. 5636, 1984.
7. Tsai, D. H. *Chemistry and Physics of Energetic Materials*. Pp. 195–227, Kluwer Academic Press, S. N. Bulusu (editor), Netherlands, 1990.
8. Peyrard, M., S. Odier, E. Lavenir, and J. M. Schnur. *Journal of Applied Physics*. Vol. 57, p. 2626, 1985.
9. Peyrard, M., S. Odier, E. Oran, J. Boris, and J. Schnur. *Physical Review B*. Vol. 33, p. 2350, 1986.
10. Lambrakos, S. G., M. Peyrard, E. S. Oran, and J. P. Boris. *Physical Review B*. Vol. 39, p. 993, 1989.
11. Maffre, P., and M. Peyrard. *Physical Review B*. Vol. 45, p. 9551, 1992.
12. Kawakatsu, T., T. Matsuda, and A. Ueda. *Journal of the Physical Society of Japan*. Vol. 57, p. 1191, 1988.
13. Kawakatsu, T., and A. Ueda. *Journal of the Physical Society of Japan*. Vol. 57, p. 2955, 1988.
14. Kawakatsu, T., and A. Ueda. *Journal of the Physical Society of Japan*. Vol. 58, p. 831, 1989.
15. Elert, M. L., D. M. Deaven, D. W. Brenner, and C. T. White. *Physical Review B*. Vol. 39, p. 1453, 1989.

16. White, C. T., D. H. Robertson, M. L. Elert, and D. W. Brenner. *Microscopic Simulations of Complex Hydrodynamic Phenomena*. Pp. 111–123, New York: Plenum Press, M. Mareschal and B. L. Holian (editors), 1992.
17. Brenner, D. W., D. H. Robertson, M. L. Elert, and C. T. White. *Physical Review Letters*. Vol. 70, p. 2174, 1993.
18. Brenner, D. W., D. H. Robertson, M. L. Elert, and C. T. White. *Physical Review Letters*. Vol. 76, p. 2202, 1996.
19. Soulard, L. "Decomposition, Combustion and Detonation Chemistry of Energetic Materials." *Materials Research Society Symposium Proceedings*, vol. 418, p. 293, T. B. Brill, T. P. Russell, W. C. Tao, and R. B. Wardle (editors), Materials Research Society, Pittsburgh, PA, 1995.
20. Rice, B. M., W. Mattson, J. Grosh, and S. F. Trevino. *Physical Review E*. Vol. 53, p. 611, 1996.
21. Rice, B. M., W. Mattson, J. Grosh, and S. F. Trevino. *Physical Review E*. Vol. 53, p. 623, 1996.
22. Haskins, P. J., and M. D. Cook. *Proceedings of the American Physical Society Topical Conference on Shock Compression of Condensed Matter*. Pp. 1341–1344, Colorado Springs, CO, 1993.
23. Haskins, P. J., and M. D. Cook. *Proceedings of the APS Topical Conference on Shock Compression of Condensed Matter*. Pp. 195–198, Seattle, WA, 1995.
24. Barrett, J. J. C., D. H. Robertson, D. W. Brenner, and C. T. White. "Decomposition, Combustion and Detonation Chemistry of Energetic Materials." *Materials Research Society Symposium Proceedings*, vol. 418, p. 301, T. B. Brill, T. P. Russell, W. C. Tao, and R. B. Wardle (editors), Materials Research Society, Pittsburgh, PA, 1995.
25. White, C. T., J. J. C. Barrett, J. W. Mintmire, M. L. Elert, and D. H. Robertson. "Decomposition, Combustion and Detonation Chemistry of Energetic Materials." *Materials Research Society Symposium Proceedings*, vol. 418, p. 277, T. B. Brill, T. P. Russell, W. C. Tao, and R. B. Wardle (editors), Materials Research Society, Pittsburgh, PA, 1995.
26. Tersoff, J. *Physical Review Letters*. Vol. 61, p. 2879, 1988.
27. Tersoff, J. *Physical Review B*. Vol. 39, p. 5566, 1989.
28. Hall, T. N., and J. R. Holden. "Explosion Effects and Properties—Part III. Properties of Explosives and Explosive Composition." *Navy Explosives Handbook*, p. 8-1, MP-88-116, Naval Surface Weapons Center, October 1988.

NO. OF COPIES	ORGANIZATION
2	DEFENSE TECHNICAL INFORMATION CENTER DTIC DDA 8725 JOHN J KINGMAN RD STE 0944 FT BELVOIR VA 22060-6218
1	HQDA DAMO FDQ DENNIS SCHMIDT 400 ARMY PENTAGON WASHINGTON DC 20310-0460
1	DPTY ASSIST SCY FOR R&T SARD TT F MILTON RM 3EA79 THE PENTAGON WASHINGTON DC 20310-0103
1	OSD OUSD(A&T)/ODDDR&E(R) R J TREW THE PENTAGON WASHINGTON DC 20301-7100
1	CECOM SP & TRRSTRL COMMCTN DIV AMSEL RD ST MC M H SOICHER FT MONMOUTH NJ 07703-5203
1	PRIN DPTY FOR TCHNLGY HQ US ARMY MATCOM AMCDCG T M FISETTE 5001 EISENHOWER AVE ALEXANDRIA VA 22333-0001
1	DPTY CG FOR RDE HQ US ARMY MATCOM AMCRD BG BEAUCHAMP 5001 EISENHOWER AVE ALEXANDRIA VA 22333-0001
1	INST FOR ADVNCD TCHNLGY THE UNIV OF TEXAS AT AUSTIN PO BOX 202797 AUSTIN TX 78720-2797

NO. OF COPIES	ORGANIZATION
1	GPS JOINT PROG OFC DIR COL J CLAY 2435 VELA WAY STE 1613 LOS ANGELES AFB CA 90245-5500
3	DARPA L STOTTS J PENNELLA B KASPAR 3701 N FAIRFAX DR ARLINGTON VA 22203-1714
1	US MILITARY ACADEMY MATH SCI CTR OF EXCELLENCE DEPT OF MATHEMATICAL SCI MDN A MAJ DON ENGEN THAYER HALL WEST POINT NY 10996-1786
1	DIRECTOR US ARMY RESEARCH LAB AMSRL CS AL TP 2800 POWDER MILL RD ADELPHI MD 20783-1145
1	DIRECTOR US ARMY RESEARCH LAB AMSRL CS AL TA 2800 POWDER MILL RD ADELPHI MD 20783-1145
3	DIRECTOR US ARMY RESEARCH LAB AMSRL CI LL 2800 POWDER MILL RD ADELPHI MD 20783-1145
	<u>ABERDEEN PROVING GROUND</u>
4	DIR USARL AMSRL CI LP (305)

<u>NO. OF COPIES</u>	<u>ORGANIZATION</u>	<u>NO. OF COPIES</u>	<u>ORGANIZATION</u>
1	HQDA SARD TT MR J APPEL WASH DC 20310-0103	2	COMMANDER US ARMY MISSILE COMMAND AMSMI RD PR E A R MAYKUT AMSMI RD PR P R BETTS REDSTONE ARSENAL AL 35898
1	HQDA OASA RDA DR C H CHURCH PENTAGON ROOM 3E486 WASH DC 20310-0103	1	OFFICE OF NAVAL RESEARCH DEPARTMENT OF THE NAVY R S MILLER CODE 432 800 N QUINCY STREET ARLINGTON VA 22217
4	COMMANDER US ARMY RESEARCH OFC R GHIRARDELLI D MANN R SINGLETON R SHAW P O BOX 12211 RESEARCH TRIANGLE PARK NC 27709-2211	1	COMMANDER NAVAL AIR SYSTEMS COMMAND J RAMNARACE AIR-54111C WASHINGTON DC 20360
1	DIRECTOR ARMY RESEARCH OFFICE AMXRO RT IP LIB SRVCS P O BOX 12211 RESEARCH TRIANGLE PARK NC 27709-2211	2	COMMANDER NSWC R BERNECKER R-13 G B WILMOT R-16 SILVER SPRING MD 20903-5000
2	COMMANDER US ARMY ARDEC AMSTA AR AEE B D S DOWNS PICATINNY ARSENAL NJ 07806-5000	5	COMMANDER NAVAL RSRCH LAB M C LIN J MCDONALD E ORAN J SHNUR R J DOYLE CODE 6110 WASHINGTON DC 20375
2	COMMANDER US ARMY ARDEC AMSTA AR AEE J A LANNON PICATINNY ARSENAL NJ 07806-5000	2	COMMANDER NAVAL WEAPONS CENTER T BOGGS CODE 388 T PARR CODE 3895 CHINA LAKE CA 93555-6001
1	COMMANDER US ARMY ARDEC AMSTA AR AEE BR L HARRIS PICATINNY ARSENAL NJ 07806-5000	1	SUPERINTENDENT NAVAL POSTGRDTE SCHL DEPT OF AERONAUTICS D W NETZER MONTEREY CA 93940
		3	AL LSCF R CORLEY R GEISLER J LEVINE EDWARDS AFB CA 93523-5000

NO. OF
COPIES ORGANIZATION

1 AFOSR
J M TISHKOFF
BOLLING AIR FORCE BASE
WASHINGTON DC 20332

1 OSD SDIO IST
L CAVENY
PENTAGON
WASHINGTON DC 20301-7100

1 COMMANDANT
USAFAS
ATSF TSM CN
FORT SILL OK 73503-5600

1 UNIV OF DAYTON RSRCH INST
D CAMPBELL
AL PAP
EDWARDS AFB CA 93523

1 NASA
LANGLEY RESEARCH CENTER
LANGLEY STATION
G B NORTHAM MS 168
HAMPTON VA 23365

4 NTNL BUREAU OF STNDRDS
J HASTIE
M JACOX
T KASHIWAGI
H SEMERJIAN
US DEPT OF COMMERCE
WASHINGTON DC 20234

2 DIRECTOR
LLNL
C WESTBROOK
W TAO MS L 282
P O BOX 808
LIVERMORE CA 94550

1 DIRECTOR
LOS ALAMOS NATIONAL LAB
B NICHOLS T7 MS-B284
P O BOX 1663
LOS ALAMOS NM 87545

NO. OF
COPIES ORGANIZATION

2 PRINCETON COMBUSTION
RSRCH LABORATORIES INC
N A MESSINA
M SUMMERFIELD
PRINCETON CORPORATE PLAZA
BLDG IV SUITE 119
11 DEERPARK DRIVE
MONMOUTH JUNCTION NJ 08852

3 DIRECTOR
SANDIA NATIONAL LABS
DIVISION 8354
S JOHNSTON
P MATTERN
D STEPHENSON
LIVERMORE CA 94550

1 BRIGHAM YOUNG UNIVERSITY
DEPT OF CHMCL ENGNRNG
M W BECKSTEAD
PROVO UT 84058

1 CALIFORNIA INST OF TECH
JET PROPULSION LAB
L STRAND MS 125 224
4800 OAK GROVE DRIVE
PASADENA CA 91109

1 CALIFORNIA INSTITUTE OF
TECHNOLOGY
F E C CULICK MC 301-46
204 KARMAN LAB
PASADENA CA 91125

1 UNIV OF CALIFORNIA
LOS ALAMOS SCNTFC LAB
P O BOX 1663
MAIL STOP B216
LOS ALAMOS NM 87545

1 UNIV OF CA BERKELEY
CHEMISTRY DEPARMENT
C BRADLEY MOORE
211 LEWIS HALL
BERKELEY CA 94720

1 UNIV OF CA SAN DIEGO
F A WILLIAMS
AMES B010
LA JOLLA CA 92093

<u>NO. OF COPIES</u>	<u>ORGANIZATION</u>
2	UNIV OF CA SANTA BARBARA QUANTUM INSTITUTE K SCHOFIELD M STEINBERG SANTA BARBARA CA 93106
1	UNIV OF CO AT BOULDER ENGINEERING CENTER J DAILY CAMPUS BOX 427 BOULDER CO 80309-0427
3	UNIV OF SOUTHERN CA DEPT OF CHEMISTRY R BEAUDET S BENSON C WITTIG LOS ANGELES CA 90007
1	CORNELL UNIVERSITY DEPT OF CHEMISTRY T A COOL BAKER LABORATORY ITHACA NY 14853
1	UNIV OF DELAWARE T BRILL CHEMISTRY DEPARTMENT NEWARK DE 19711
1	UNIVERSITY OF FLORIDA DEPT OF CHEMISTRY J WINEFORDNER GAINESVILLE FL 32611
3	GA INST OF TECHNOLOGY SCHL OF AERSPCE ENGNRNG E PRICE W C STRAHLE B T ZINN ATLANTA GA 30332
1	UNIVERSITY OF ILLINOIS DEPT OF MECH ENG H KRIER 144MEB 1206 W GREEN ST URBANA IL 61801

<u>NO. OF COPIES</u>	<u>ORGANIZATION</u>
1	THE JOHNS HOPKINS UNIV CPIA T W CHRISTIAN 10630 LTLE PTXNT PKWY STE 202 COLUMBIA MD 21044-3200
1	UNIVERSITY OF MICHIGAN GAS DYNAMICS LAB AEROSPACE ENGNRNG BLDG G M FAETH ANN ARBOR MI 48109-2140
1	UNIVERSITY OF MINNESOTA DEPT OF MCHNCL ENGNRNG E FLETCHER MINNEAPOLIS MN 55455
4	PA STATE UNIVERSITY DEPT OF MCHNCL ENGNRNG K KUO M MICCI S THYNELL V YANG UNIVERSITY PARK PA 16802
2	PRINCETON UNIVERSITY FORRESTAL CAMPUS LIB K BREZINSKY I GLASSMAN P O BOX 710 PRINCETON NJ 08540
1	PURDUE UNIVERSITY SCHOOL OF AERO & ASTRO J R OSBORN GRISSOM HALL WEST LAFAYETTE IN 47906
1	PURDUE UNIVERSITY DEPT OF CHEMISTRY E GRANT WEST LAFAYETTE IN 47906
2	PURDUE UNIVERSITY SCHL OF MCHNCL ENGNRNG N M LAURENDEAU S N B MURTHY TSPC CHAFFEE HALL WEST LAFAYETTE IN 47906

<u>NO. OF COPIES</u>	<u>ORGANIZATION</u>
1	RENSSELAER PLYTCHNC INST DEPT OF CHMCL ENGNRNG A FONTIJN TROY NY 12181
1	STANFORD UNIVERSITY DEPT OF MCHNCL ENGNRNG R HANSON STANFORD CA 94305
1	UNIVERSITY OF TEXAS DEPT OF CHEMISTRY W GARDINER AUSTIN TX 78712
1	VIRGINIA PLYTCHNC INST AND STATE UNIVERSITY A SCHETZ BLACKSBURG VA 24061
1	APPLIED COMBUSTION TECHNOLOGY INC A M VARNEY P O BOX 607885 ORLANDO FL 32860
2	APPLIED MCHNCS REVIEWS THE AMERICAN SOCIETY OF MECHANICAL ENGINEERS R E WHITE A B WENZEL 345 E 47TH STREET NEW YORK NY 10017
1	BATTELLE TWSTIAC 505 KING AVENUE COLUMBUS OH 43201-2693
1	COHEN PRFSSNL SERVICES N S COHEN 141 CHANNING STREET REDLANDS CA 92373
1	EXXON RSRCH & ENGRNG CO A DEAN ROUTE 22E ANNANDALE NJ 08801

<u>NO. OF COPIES</u>	<u>ORGANIZATION</u>
1	GENERAL APPLIED SCIENCE LABORATORIES INC 77 RAYNOR AVENUE RONKONKAMA NY 11779-6649
1	GENERAL MOTORS RSCH LABS PHYSCL CHMSTRY DEPT T SLOANE WARREN MI 48090-9055
2	HERCULES INC ALLEGHENY BALLISTICS LAB W B WALKUP E A YOUNT P O BOX 210 ROCKET CENTER WV 26726
1	HERCULES INC R V CARTWRIGHT 100 HOWARD BLVD KENVIL NJ 07847
1	ALLIANT TECHSYSTEMS INC MARINE SYSTEMS GROUP D E BRODEN MS MN50-2000 600 2ND STREET NE HOPKINS MN 55343
1	ALLIANT TECHSYSTEMS INC R E TOMPKINS MN 11 2720 600 SECOND ST NORTH HOPKINS MN 55343
1	IBM CORPORATION A C TAM RESEARCH DIVISION 5600 COTTLE ROAD SAN JOSE CA 95193
1	IIT RESEARCH INSTITUTE R F REMALY 10 WEST 35TH STREET CHICAGO IL 60616
1	LOCKHEED MSLS & SPACE CO GEORGE LO 3251 HANOVER STREET DEPT 52-35 B204 2 PALO ALTO CA 94304

<u>NO. OF</u> <u>COPIES</u>	<u>ORGANIZATION</u>	<u>NO. OF</u> <u>COPIES</u>	<u>ORGANIZATION</u>
1	OLIN ORDNANCE V MCDONALD LIBRARY P O BOX 222 ST MARKS FL 32355-0222	3	THIOKOL CORPORATION ELKTON DIVISION R BIDDLE R WILLER TECH LIB P O BOX 241 ELKTON MD 21921
1	PAUL GOUGH ASSOCIATES INC P S GOUGH 1048 SOUTH STREET PORTSMOUTH NH 03801-5423	3	THIOKOL CORPORATION WASATCH DIVISION S J BENNETT P O BOX 524 BRIGHAM CITY UT 84302
1	HUGHES AIRCRAFT COMPANY T E WARD 8433 FALLBROOK AVENUE CANOGA PARK CA 91303	1	UNITED TCHNLGS RSRCH CTR A C ECKBRETH EAST HARTFORD CT 06108
1	ROCKWELL INTRNTNL CORP ROCKETDYNE DIVISION J E FLANAGAN HB02 6633 CANOGA AVENUE CANOGA PARK CA 91304	1	UNITED TECHNOLOGIES CORP CHEMICAL SYSTEMS DIVISION R R MILLER P O BOX 49028 SAN JOSE CA 95161-9028
1	SCIENCE APPLICATIONS INC R B EDELMAN 23146 CUMORAH CREST WOODLAND HILLS CA 91364	1	UNIVERSAL PRPLSN CO H J MCSPADDEN 25401 NORTH CENTRAL AVE PHOENIX AZ 85027-7837
3	SRI INTERNATIONAL G SMITH D CROSLEY D GOLDEN 333 RAVENSWOOD AVENUE MENLO PARK CA 94025	1	VERITAY TECHNOLOGY INC E B FISHER 4845 MILLERSPORT HWY P O BOX 305 EAST AMHERST NY 14051-0305
1	STEVENS INST OF TECH DAVIDSON LABORATORY R MCALEVY III HOBOKEN NJ 07030	1	FREEDMAN ASSOCIATES E FREEDMAN 2411 DIANA ROAD BALTIMORE MD 21209-1525
1	NYMA INC LERC GROUP R J LOCKE MS SVR 2 2001 AEROSPACE PKWY BROOK PARK OH 44142	1	ALLIANT TECHSYSTEMS INC J BODE 600 SECOND ST NE HOPKINS MN 55343
		1	ALLIANT TECHSYSTEMS INC C CANDLAND 600 SECOND ST NE HOPKINS MN 55343

<u>NO. OF</u> <u>COPIES</u>	<u>ORGANIZATION</u>	<u>NO. OF</u> <u>COPIES</u>	<u>ORGANIZATION</u>
1	ALLIANT TECHSYSTEMS INC L OSGOOD 600 SECOND ST NE HOPKINS MN 55343		<u>ABERDEEN PROVING GROUND</u>
1	ALLIANT TECHSYSTEMS INC R BURETTA 600 SECOND ST NE HOPKINS MN 55343	41	DIR, USARL AMSRL-WM-B, A.W. HORST AMSRL-WM-BD, B.E. FORCH G.F. ADAMS W.R. ANDERSON R.A. BEYER S.W. BUNTE C.F. CHABALOWSKI S. COLEMAN A. COHEN R. CUMPTON R. DANIEL D. DEVYNCK R.A. FIFER J.M. HEIMERL B.E. HOMAN A. JUHASZ A.J. KOTLAR R. KRANZE E. LANCASTER W.F. MCBRATNEY K.L. MCNESBY M. MCQUAID N.E. MEAGHER M.S. MILLER A.W. MIZIOLEK J.B. MORRIS J.E. NEWBERRY S.V. PAI R.A. PESCE-RODRIGUEZ J. RASIMAS P. REEVES B.M. RICE P. SAEGAR R.C. SAUSA M.A. SCHROEDER R. SCHWEITZER L.D. SEGER J.A. VANDERHOFF D. VENIZELOS A. WHREN H.L. WILLIAMS
1	ALLIANT TECHSYSTEMS INC R BECKER 600 SECOND ST NE HOPKINS MN 55343		
1	ALLIANT TECHSYSTEMS INC M SWENSON 600 SECOND ST NE HOPKINS MN 55343		
1	BENET LABORATORIES SAM SOPOK AMSTA AR CCB B WATERVLIET NY 12189		

INTENTIONALLY LEFT BLANK.

REPORT DOCUMENTATION PAGE			Form Approved OMB No. 0704-0188	
<small>Public reporting burden for this collection of information is estimated to average 1 hour per response, including the time for reviewing instructions, searching existing data sources, gathering and maintaining the data needed, and completing and reviewing the collection of information. Send comments regarding this burden estimate or any other aspect of this collection of information, including suggestions for reducing this burden, to Washington Headquarters Services, Directorate for Information Operations and Reports, 1215 Jefferson Davis Highway, Suite 1204, Arlington, VA 22202-4302, and to the Office of Management and Budget, Paperwork Reduction Project (0704-0188), Washington, DC 20503.</small>				
1. AGENCY USE ONLY (Leave blank)		2. REPORT DATE August 1998		3. REPORT TYPE AND DATES COVERED Final, Jan - Sep 97
4. TITLE AND SUBTITLE Molecular Dynamics Investigation of the Desensitization of Detonable Material			5. FUNDING NUMBERS 1L161102AH43	
6. AUTHOR(S) Betsy M. Rice, William Mattson, and Samuel F. Trevino				
7. PERFORMING ORGANIZATION NAME(S) AND ADDRESS(ES) U.S. Army Research Laboratory ATTN: AMSRL-WM-BD Aberdeen Proving Ground, MD 21005-5066			8. PERFORMING ORGANIZATION REPORT NUMBER ARL-TR-1744	
9. SPONSORING/MONITORING AGENCY NAME(S) AND ADDRESS(ES)			10. SPONSORING/MONITORING AGENCY REPORT NUMBER	
11. SUPPLEMENTARY NOTES				
12a. DISTRIBUTION/AVAILABILITY STATEMENT Approved for public release; distribution is unlimited			12b. DISTRIBUTION CODE	
13. ABSTRACT (Maximum 200 words) <p>A molecular dynamics investigation of the effects of a diluent on the detonation of a model crystalline explosive is presented. The diluent, a heavy material that cannot exothermally react with any species of the system, is inserted into the crystalline explosive in two ways. The first series of simulations investigates the attenuation of the energy of a detonation wave in a pure explosive after it encounters a small layer of crystalline diluent that has been inserted into the lattice of the pure explosive. After the shock wave has traversed the diluent layer, it reenters pure explosive. Unsupported detonation is not reestablished unless the energy of the detonation wave exceeds a threshold value. The second series of simulations investigates detonation of solid solutions of different concentrations of explosive and diluent. For both types of simulations, the key to reestablishing or reaching unsupported detonation is the attainment of a critical number density behind the shock front. Once this critical density is reached, the explosive molecules transition to an atomic phase. This is the first step in the reaction mechanism that leads to the heat release that sustains the detonation. The reactive fragments formed from the atomization of the heteronuclear reactants subsequently combine with new partners, with homonuclear product formation exothermally favored.</p>				
14. SUBJECT TERMS molecular dynamics, detonation, explosives			15. NUMBER OF PAGES 29	
			16. PRICE CODE	
17. SECURITY CLASSIFICATION OF REPORT UNCLASSIFIED	18. SECURITY CLASSIFICATION OF THIS PAGE UNCLASSIFIED	19. SECURITY CLASSIFICATION OF ABSTRACT UNCLASSIFIED	20. LIMITATION OF ABSTRACT UL	

INTENTIONALLY LEFT BLANK.

USER EVALUATION SHEET/CHANGE OF ADDRESS

This Laboratory undertakes a continuing effort to improve the quality of the reports it publishes. Your comments/answers to the items/questions below will aid us in our efforts.

1. ARL Report Number/Author ARL-TR-1744 (Rice) Date of Report August 1998

2. Date Report Received _____

3. Does this report satisfy a need? (Comment on purpose, related project, or other area of interest for which the report will be used.) _____

4. Specifically, how is the report being used? (Information source, design data, procedure, source of ideas, etc.) _____

5. Has the information in this report led to any quantitative savings as far as man-hours or dollars saved, operating costs avoided, or efficiencies achieved, etc? If so, please elaborate. _____

6. General Comments. What do you think should be changed to improve future reports? (Indicate changes to organization, technical content, format, etc.) _____

CURRENT
ADDRESS

Organization

Name

E-mail Name

Street or P.O. Box No.

City, State, Zip Code

7. If indicating a Change of Address or Address Correction, please provide the Current or Correct address above and the Old or Incorrect address below.

OLD
ADDRESS

Organization

Name

Street or P.O. Box No.

City, State, Zip Code

(Remove this sheet, fold as indicated, tape closed, and mail.)
(DO NOT STAPLE)